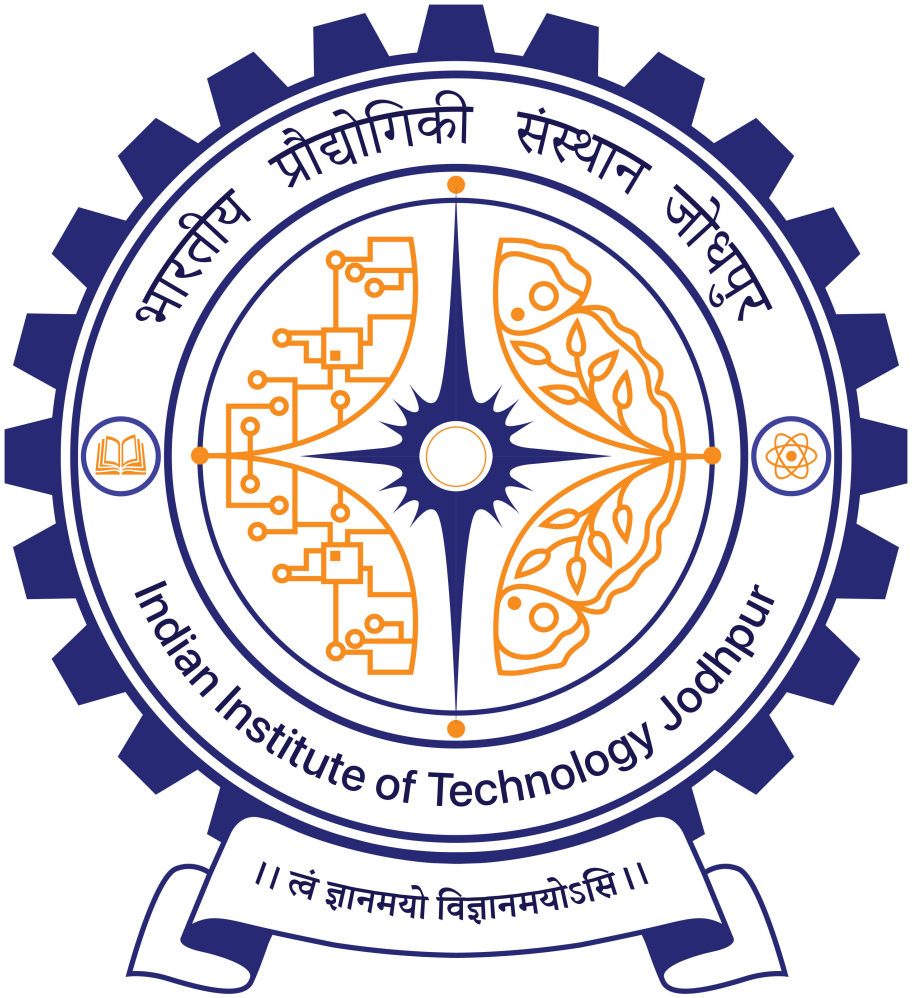

Analysis of Hand Segmentation in the Wild

Supervisor: Dr.Avinash Sharma

GitHub Repo

Team Member	Roll Number
Deepak Bhatter	B22EE022
Aditya Kumar	B22ME004
Mayank Agrawal	B22CS084

Contents

1 Introduction **1**
- 1.1 Introduction . . . 1
  - 1.1.1 Contributions (summary) . . . 1
- 1.2 Datasets Used . . . 2
  - 1.2.1 Dataset descriptions . . . 2
- 1.3 Methodology and Architecture . . . 2
  - 1.3.1 Problem formulation . . . 2
  - 1.3.2 Model choice: RefineNet-Res101 . . . 3
  - 1.3.3 RefineNet building blocks (detailed) . . . 3
  - 1.3.4 Training details . . . 4
  - 1.3.5 Conditional Random Fields (CRF) refinement . . . 4
- 1.4 Experiments and Results . . . 5
  - 1.4.1 Evaluation metrics . . . 5
  - 1.4.2 Per-dataset segmentation results and cross-dataset evaluation . . . 5
  - 1.4.3 CRF refinement: qualitative vs quantitative effects . . . 6
- 1.5 Additional Analyses by the Authors . . . 7
- 1.6 Discussion . . . 7
- 1.7 Conclusions . . . 8

2 Initial Experiment: DeepLabV3-ResNet50 **9**
- 2.1 Overview . . . 9
- 2.2 Implementation Details . . . 9
- 2.3 Results and Observations . . . 10
- 2.4 Demo Video . . . 10
- 2.5 Summary . . . 10

3 GrabCut **11**
- 3.1 Overview of Methodology . . . 11
- 3.2 YOLOv8 Nano Architecture . . . 11
- 3.3 Datasets Used for Training . . . 12
- 3.4 Results and Analysis . . . 15
- 3.5 Discussion . . . 16

4 RefineNet Implementation **20**
- 4.1 Overview of the Implementation Pipeline . . . 20
- 4.2 Step 1: Pretraining on Pascal Parts Dataset . . . 20
  - 4.2.1 Data Extraction and Preprocessing . . . 20
  - 4.2.2 Pretraining Setup . . . 22

4.3 Step 2: Fine-Tuning on Hand Segmentation Datasets 22
4.3.1 Training Details 22
4.3.2 Batch Size Comparison 22
4.4 Step 3: Cross-Dataset Evaluation 22
4.5 Step 4: Visual Results 23
4.6 Challenges Faced 26
4.7 Conclusion 26

Chapter 1

Introduction

This chapter provides a comprehensive, self-contained explanation of the paper "**Analysis of Hand Segmentation in the Wild**" by Aisha Urooj Khan and Ali Borji . It describes the motivation, the datasets used and created by the authors, the methodology (network architecture, training recipes, and refinement techniques), and a thorough presentation of experimental results and analysis.

1.1 Introduction

Hand segmentation in first-person (egocentric) videos is a core problem for many applications including activity recognition, augmented reality, robotics, and human–computer interaction. Unlike third-person videos, egocentric data exhibit:

- rapid viewpoint and illumination changes,
- strong camera motion,
- frequent occlusions and hand-object interactions,
- absence of the camera-wearer's face or body as a localization cue.

The studied paper focuses on pixel-level hand segmentation (binary semantic segmentation: *hand* vs *non-hand*). The authors revisit prior approaches and evaluate modern semantic segmentation networks, identifying and fine-tuning *RefineNet-Res101* as a top performer for this task. They also introduce three new datasets aimed at realistic scenarios and analyze cross-dataset generalization, the role of Conditional Random Fields (CRFs) for refinement, and the downstream utility of hand maps for activity recognition.

1.1.1 Contributions (summary)

1. Fine-tuning RefineNet-Res101 for pixel-wise hand segmentation and showing substantial improvements over prior baselines (e.g., Bambach et al.).
2. Introducing three datasets: **EgoYouTubeHands (EYTH)**, **HandOverFace (HOF)**, and **EgoHands+** (fine-level action annotations).
3. Systematic cross-dataset generalization analysis and evaluation of CRF refinements.
4. Demonstrating the benefit of accurate hand maps for coarse and fine-level activity recognition.

1.2 Datasets Used

The paper uses five datasets (two established and three newly contributed).

Table 1.1: Dataset statistics used in the study. "1st-P" and "3rd-P" denote first-person and third-person hands respectively.

Dataset	Frames	Hand instances	1st-P instances	3rd-P instances
EgoHands (Bambach et al.)	4,800	15,053	5,976	9,077
EgoYouTubeHands (EYTH)	1,290	2,600	1,811	789
GTEA	663	1,231	1,231	—
HandOverFace (HOF)	300	507	—	507
EgoHands+ (action labels)	800	—	—	—

1.2.1 Dataset descriptions

EgoHands The EgoHands dataset contains 48 Google Glass videos of two people interacting (activities: puzzle, cards, jenga, chess) captured in three environments. It contains ∼15k hand instances with pixel-level annotations (hands annotated until the wrist). It is commonly used as a standard egocentric hand segmentation benchmark.

EgoYouTubeHands (EYTH) The authors collected three unconstrained first-person videos from YouTube, annotated every 5^{th} frame to build a dataset of ∼1290 frames (2600 hand instances). It contains diverse scenes and large variations in lighting, scale and occlusion, making it especially challenging and valuable for generalization.

GTEA Georgia Tech Egocentric Activity dataset with cooking actions; used here for hand segmentation (663 annotated frames). It is captured in a constrained, static environment and thus less varied than EYTH.

HandOverFace (HOF) A small collection (300 images) of faces occluded by hands, collected from the web to study the effect of similar skin appearance (hand vs face) on segmentation.

EgoHands+ A subset of EgoHands with fine-level hand/pixel action labels (16 action labels; used to study fine-grained action recognition from single hand instances). The authors chose 8 most frequent actions for classification experiments.

1.3 Methodology and Architecture

1.3.1 Problem formulation

Hand segmentation is treated as a *binary semantic segmentation* problem: each pixel is classified as `hand` or `non-hand`. All training and evaluation metrics adopt standard dense-prediction metrics: mean Intersection-over-Union (mIOU), mean precision, and mean recall (pixel-level).

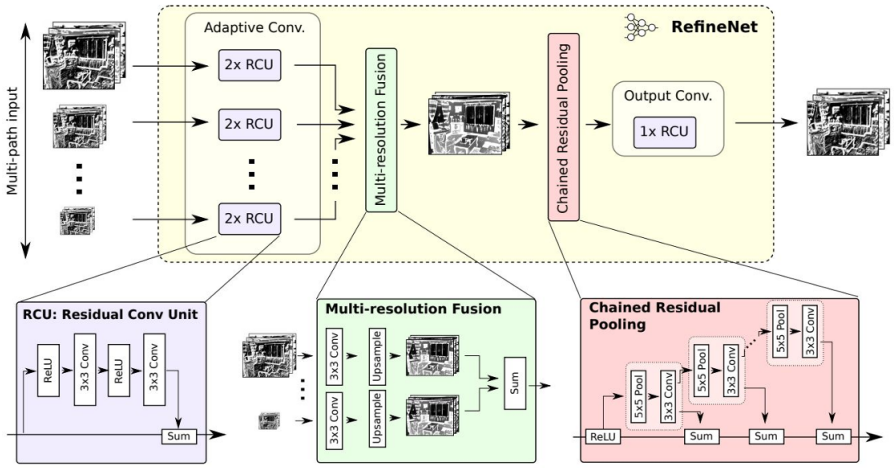

(a) Complete Refinement Network

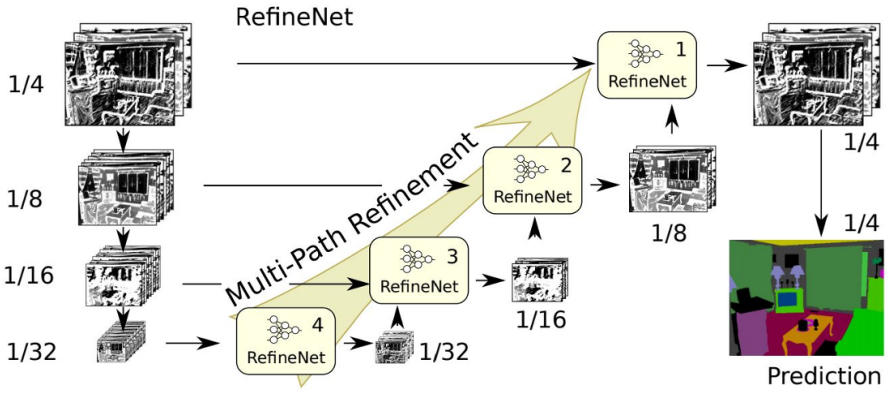

(b) RefineNet Architecture

1.3.2 Model choice: RefineNet-Res101

The authors selected **RefineNet** with a ResNet-101 backbone (RefineNet-Res101) for the following reasons:

- RefineNet is designed for high-resolution semantic segmentation by fusing multi-level features from different ResNet stages.
- It provides multi-path refinement blocks that combine contextual, coarse-level features with high-resolution features to reconstruct fine spatial structures such as fingers.
- Off-the-shelf RefineNet models pretrained on PASCAL Person-Part already encode useful human-part priors, making them a strong starting point for hand segmentation.

1.3.3 RefineNet building blocks (detailed)

RefineNet employs a cascade of blocks and several novel operations; below are the main components:

- **Residual Convolution Unit (RCU):** Simplified residual blocks that refine incoming feature maps. Each RCU typically applies two convolutions with residual (identity) connections; in some implementations batch normalization is removed for simplification.
- **Multi-Resolution Fusion (MRF):** It aligns and fuses feature maps coming from different resolutions (e.g., features from ResNet conv2, conv3, conv4, conv5). When fusing, the lower-resolution maps are upsampled (usually by bilinear interpolation or learned upsampling) and combined via summation or concatenation followed by a convolution.
- **Chained Residual Pooling (CRP):** A chain of pooling blocks (each: pooling $\rightarrow$ conv) that aggregates contextual information from increasing receptive fields. These pooled outputs are combined with residual connections to preserve high-frequency details.
- **Output Convolution / Final prediction:** After cascaded RefineNet blocks refine multi-level features, a final convolution layer produces dense per-pixel class logits followed by softmax for classification.

1.3.4 Training details

The paper's training recipe (summary):

- **Pretraining:** Use RefineNet-Res101 pretrained on Pascal Person-Part (helps because person-part priors include hands).
- **Output classes:** Convert to a 2-class problem: `hand` and `no-hand` by replacing the final classification layer with a binary dense predictor.
- **Learning rates:** A base learning rate of 5×10^{-5} for the pretrained layers, while the new classification layer uses an increased LR factor.
- **Multi-scale evaluation:** Evaluate using multi-scale inference with scales $[0.6, 0.8, 1.0]$ (average or max fusion), which consistently gave better performance than single-scale inference.
- **Optimization:** Models are fine-tuned until convergence; the number of epochs used per dataset (as reported) are: EgoHands (80 epochs), EYTH (85 epochs), GTEA (92 epochs), HOF (61 epochs).
- **Post-processing:** Dense-CRF (fully-connected CRF) or other CRF formulations are applied on top of the RefineNet soft outputs to refine predicted masks and recover fine boundary details.

1.3.5 Conditional Random Fields (CRF) refinement

The authors applied CRF inference (pairwise and unary potentials computed from classifier outputs and image features) as a post-processing step in an attempt to better align segmentation masks with image edges and recover finger-level details. They observed:

- Qualitatively, CRF often sharpens fingers and small structures and can remove some false positives.

- Quantitatively, CRF sometimes slightly reduces mIOU (depending on dataset), but yields visually appealing improvements; the net effect varies by dataset (for GTEA the change was negligible).
- CRF helped in some occlusion cases (e.g., disambiguating overlapping hands) by enforcing spatial coherence.

1.4 Experiments and Results

This section states the key experimental findings of the paper: per-dataset segmentation results, cross-dataset generalization, analysis on small vs. large hands, CRF effects, and activity recognition experiments.

1.4.1 Evaluation metrics

The main evaluation metrics:

- **Mean Intersection over Union (mIOU)** (primary metric).
- **Mean Precision** (pixel-level).
- **Mean Recall** (pixel-level).
- **Classification accuracy** for activity recognition tasks.

1.4.2 Per-dataset segmentation results and cross-dataset evaluation

Table **??** shows RefineNet results when trained on each dataset and tested on others (rows: training dataset; columns: test dataset aggregated metrics mIOU / mRecall / mPrecision). Bold numbers indicate best result per test set (as in the original paper).

Train ↓ / Test →	EgoHands	EYTH	GTEA	HOF
EgoHands	**0.814** / 0.919 / 0.879	0.428 / 0.615 / 0.550	0.774 / 0.834 / 0.904	0.503 / 0.738 / 0.619
EYTH	0.670 / 0.768 / 0.841	**0.688** / 0.776 / 0.853	0.666 / 0.700 / 0.920	0.528 / 0.653 / 0.722
GTEA	0.152 / 0.307 / 0.204	0.440 / 0.569 / 0.614	**0.821** / 0.869 / 0.928	0.263 / 0.880 / 0.276
HOF	0.578 / 0.701 / 0.780	0.423 / 0.497 / 0.667	0.431 / 0.450 / 0.879	**0.766** / 0.882 / 0.859

Table 1.2: Hand segmentation results (RefineNet)

Key observations

- **Best within-dataset performance:** Each model performs best when trained and tested on the same dataset (diagonal values), e.g., EgoHands → EgoHands yields 0.814 mIOU.
- **EYTH generalizes best:** The model trained on EYTH (the in-the-wild YouTube dataset) generalizes relatively well to other datasets (second-best for EgoHands and HOF) — likely because EYTH contains rich diversity (lighting, scale, occlusion, social interactions).
- **GTEA generalization is poor:** Models trained on GTEA (constrained cooking environment) generalize poorly to EgoHands, EYTH and HOF — showing the limitations of datasets with restricted variability.

- **HOF utility:** Despite being small, HOF-trained models generalize better than GTEA in some cases, suggesting that repeated exposure to *similar appearance occlusions* (hand over face) helps the network disambiguate skin-like regions.

1.4.3 CRF refinement: qualitative vs quantitative effects

The authors applied a dense CRF post-processing (pairwise potentials based on color and position) to refine RefineNet predictions. Findings:

- CRF often helps visually (sharper boundaries and finger details).
- Quantitatively, CRF sometimes marginally decreases mIOU (depends on dataset). For GTEA the mIOU change was negligible (drop $\approx 0.5\%$).
- CRF can help split merged hand instances in occlusion cases by imposing spatial smoothness and edge-aware pairwise terms.

Figure 1.2 shows representative qualitative examples (replace with high-resolution results from your experiments).

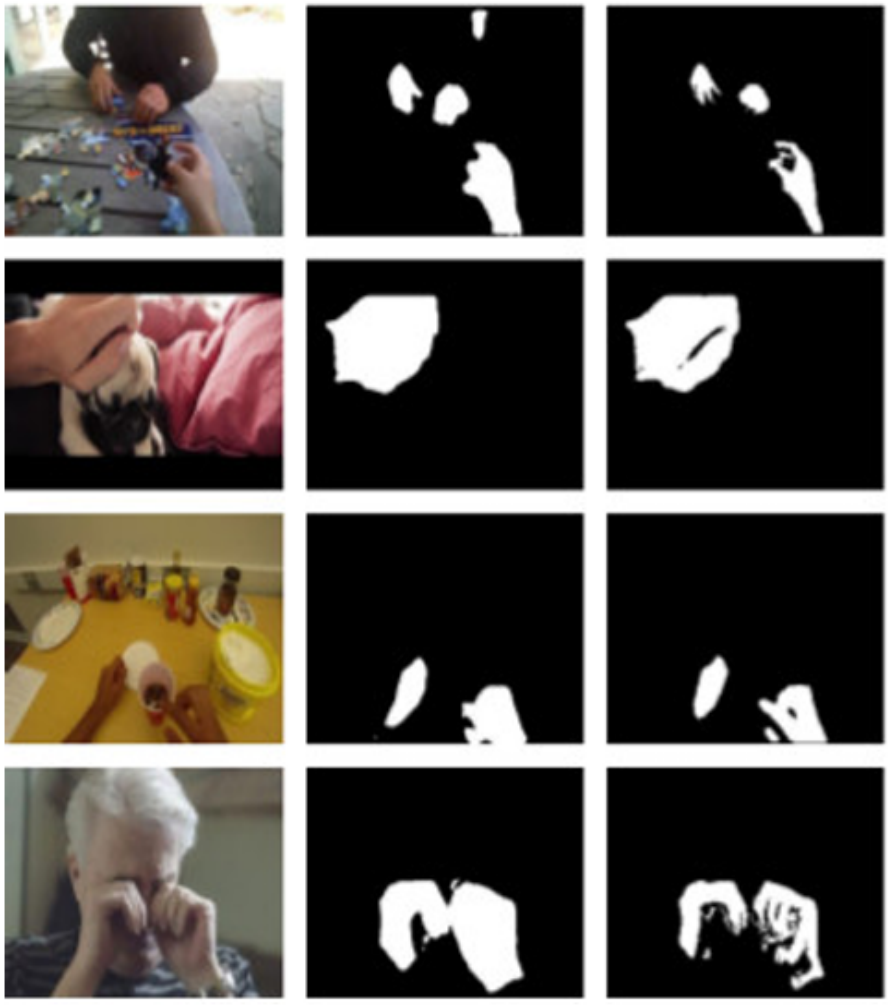

Figure 1.2: Qualitative examples showing CRF refinement

1.5 Additional Analyses by the Authors

The original RefineNet hand-segmentation paper includes two additional analyses that we were unable to reproduce due to the unavailability of required annotations and datasets.

(1) Small vs. Big Hands Analysis. The authors evaluated scale sensitivity by splitting test hands into *small* and *big* based on the relative bounding-box area (small: < 0.015, big: > 0.15; for GTEA, small: < 0.025). Their results consistently showed that small hands are more challenging across datasets, with noticeably lower mIOU, mRecall, and mPrecision compared to big hands. This highlights the inherent scale difficulty in egocentric hand segmentation.

(2) Activity and Action Recognition Using Hand Maps. The authors also investigated how improved hand maps affect downstream recognition tasks:

- **Coarse-level activity recognition** on EgoHands (cards, chess, jenga, puzzle), where better hand maps (RefineNet-FT) significantly improved accuracy over baseline hand maps, and ground-truth maps achieved the best performance.
- **Fine-level action recognition** on the EgoHands+ subset, where the combination of hand maps and object cues yielded the best results ($\sim$77

Note. These experiments require detailed activity and action annotations (e.g., frame-level activity labels, fine-grained hand–object interaction labels), which were not publicly available for our dataset. Therefore, while we report the findings from the original authors for completeness, we were unable to replicate these analyses in our work.

1.6 Discussion

Why RefineNet works well Its explicit multi-level fusion is especially helpful for hands which require both coarse contextual cues (where hands typically appear) and fine details (fingers, narrow boundaries). Pretraining on person-part datasets also helps by transferring human-part awareness.

Limitations and failure modes

- **Small hands:** Low-resolution or far-away hands yield lower mIOU.
- **Severe motion blur**: Frame blur can confuse the classifier.
- **Skin-like confusers:** Hands in front of face or other skin-colored regions cause false positives without specialized cues.
- **Hand-hand occlusions:** When hands overlap heavily, the model may merge instances.
- **Dataset bias:** Models trained on constrained datasets (e.g., GTEA) generalize poorly to in-the-wild data.

1.7 Conclusions

The paper demonstrates that:

- Modern segmentation architectures (RefineNet) significantly outperform prior pipelines for egocentric hand segmentation.
- Datasets with diverse, unconstrained conditions (EYTH) yield models that generalize better across domains.
- CRF post-processing yields qualitative improvements and can help in difficult occlusion cases but does not guarantee a quantitative mIOU increase.
- Accurate hand maps are valuable for both coarse- and fine-grained activity recognition; in particular, combining hand and object information yields substantial gains.

Chapter 2

Initial Experiment: DeepLabV3-ResNet50

In this chapter, we describe our initial attempt to replicate the hand segmentation task using a simpler architecture based on a standard **ResNet backbone** without any complex refinement modules such as those in RefineNet. This was done primarily to understand the core challenges of hand segmentation before moving to more sophisticated networks.

2.1 Overview

As a starting point, we experimented with the `DeepLabV3-ResNet50` architecture from the `torchvision.models.segmentation` library. The model was pretrained on COCO and then fine-tuned on the **EgoHands dataset**. The segmentation task was formulated as a binary classification problem (`hand` vs. `background`).

This approach was intentionally naive — the goal was to test whether a vanilla deep residual model could capture the general structure of hands without additional refinement mechanisms.

2.2 Implementation Details

The model training pipeline was implemented using **PyTorch**. The essential components of the pipeline include:

- **Backbone:** `DeepLabV3` with a `ResNet-50` encoder.
- **Classifier modification:** The last layer of the model was replaced with a 1×1 convolution producing two output channels (for hand and non-hand classes).
- **Loss function:** Cross-Entropy Loss.
- **Optimizer:** Adam optimizer with a learning rate of 1×10^{-4}.
- **Training setup:** 10 epochs with a batch size of 4 on the EgoHands processed dataset.

During training, we measured both **IoU score** and **pixel accuracy** per epoch. The model successfully converged to segment visible hand regions in most of the frames.

2.3 Results and Observations

The trained model was capable of segmenting hands in various frames of the EgoHands dataset with acceptable accuracy. However, certain limitations were clearly observed:

- The model performed reasonably well on typical egocentric frames where hands appear distinctly from the background.
- When a **face** appeared in the frame, the model often misclassified it as a hand region. This occurred because both hands and faces share similar color and texture features, and without specialized refinement modules or contextual awareness, the ResNet-based model could not distinguish them effectively.
- The model also sometimes failed under poor lighting or when the hand was too small in the frame.

(a) Hand Segmentation Result

(b) Incorrect Segmentation of Face

Despite these issues, the experiment confirmed that even a simple ResNet-based encoder-decoder architecture can learn coarse hand localization cues, which validates the feasibility of using deep CNNs for egocentric hand segmentation tasks.

2.4 Demo Video

A short demonstration video showcasing the trained model's predictions.

Hand Segmentation Demo Video

2.5 Summary

This simple experiment with **DeepLabV3-ResNet50** highlighted the strengths and weaknesses of basic residual architectures for dense prediction tasks like hand segmentation. While the network achieved reasonable segmentation performance on clear frames, it failed in ambiguous contexts (e.g., face-hand confusion). These insights motivated the exploration of more advanced architectures like **RefineNet**, which leverage multi-level feature refinement and contextual reasoning to address such issues effectively.

Chapter 3

YOLO based Hand Detection & GrabCut Segmentation

After observing the limitations of our naive ResNet-based segmentation model—particularly its confusion between hands and faces—we explored an alternate approach that combines **object detection** with **color-based segmentation**. Specifically, we used a fine-tuned **YOLOv8 Nano** model to localize hands via bounding boxes and then refined these detections into pixel-level masks using the **GrabCut** algorithm. This hybrid approach yielded promising results for most scenarios.

3.1 Overview of Methodology

The core idea was to first detect the approximate region of the hand using a lightweight detector (YOLOv8 Nano), and then refine that region using a color-based segmentation method (GrabCut). The steps are summarized below:

1. Fine-tune a YOLOv8 Nano model for hand detection on multiple datasets.
2. During inference, obtain the detected bounding box around the hand.
3. Compute the **center point** of the detected box and define a smaller region covering roughly **3% of the area** of the YOLO box.
4. Use this smaller box as a **foreground seed region** for GrabCut, while the rest of the image is initialized as probable or definite background.
5. Apply the GrabCut segmentation algorithm on the image.

This process effectively uses the YOLO detector to provide localization cues, while GrabCut performs color-based fine segmentation inside the detected region.

3.2 YOLOv8 Nano Architecture

The YOLOv8 Nano model belongs to the YOLOv8 family introduced by Ultralytics, designed for speed and compactness. It follows a standard one-stage detector structure comprising three main parts:

- **Backbone:** A modified **CSPDarkNet** architecture that extracts multiscale features from the image. The Nano version reduces depth and width multipliers for efficiency, resulting in fewer parameters ($\sim$ 3.2M).
- **Neck:** The **PAN-FPN (Path Aggregation Network)** integrates low-level spatial information with high-level semantic context. It enhances localization while maintaining efficiency through concatenation and upsampling layers.
- **Head:** A decoupled detection head that predicts bounding boxes, confidence scores, and class probabilities simultaneously at multiple scales. The head outputs anchor-free predictions using `sigmoid` activations, allowing precise object localization.

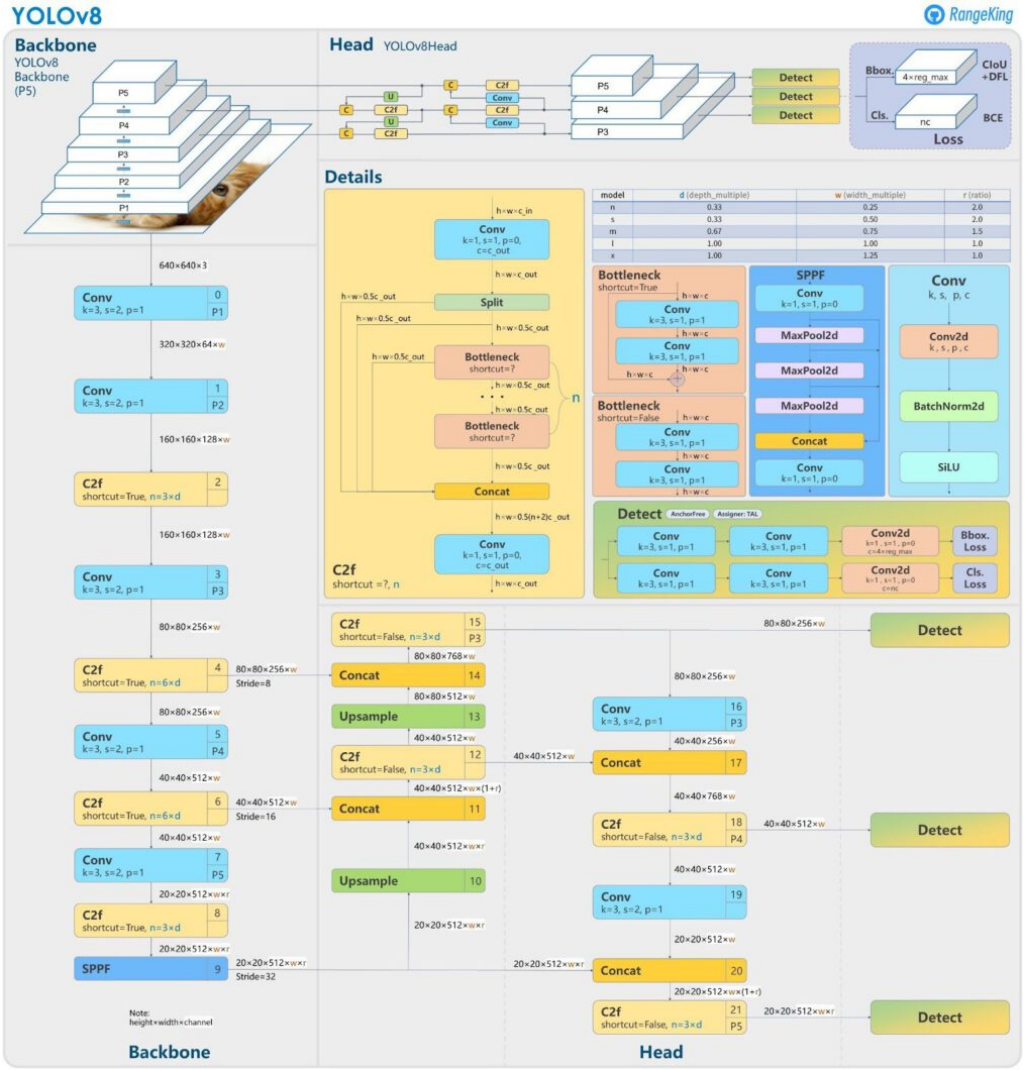

Figure 3.1: YOLOv8 Nano architecture overview

3.3 Datasets Used for Training

To achieve robust detection performance, we fine-tuned YOLOv8 Nano on multiple publicly available hand detection datasets:

- **Hands Gesture** — https://universe.roboflow.com/sonu-frtzd/hand-7hx79-rxqsz/dataset/1

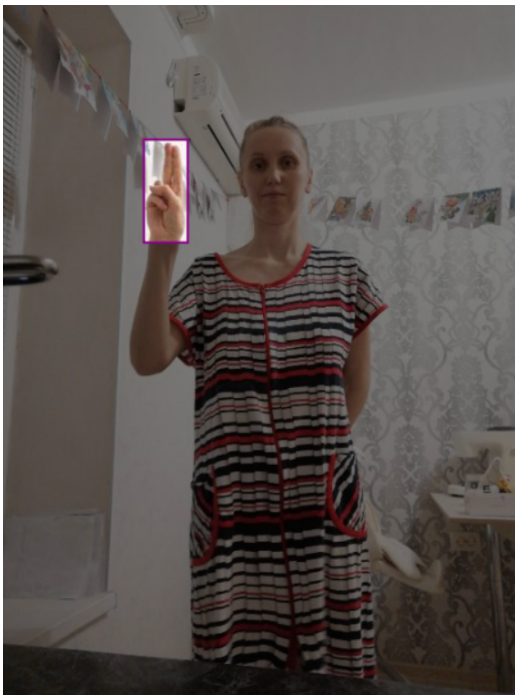

- **Hand Object Detection** — https://universe.roboflow.com/sonu-frtzd/hand-detection-5gzvh-ntp0h/dataset/1

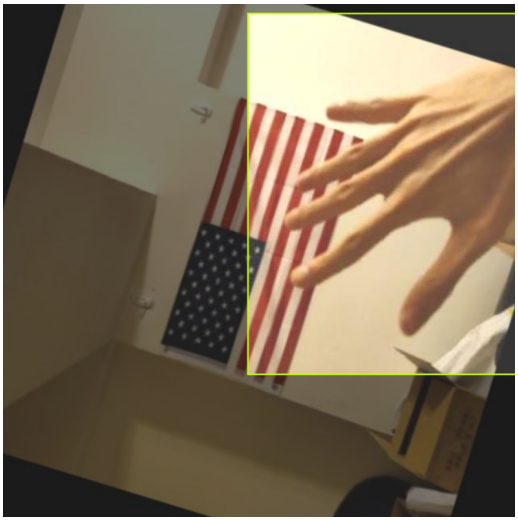

- **Hand Gesture** — https://universe.roboflow.com/sonu-frtzd/hand-bo3ot-jhr1r/dataset/1

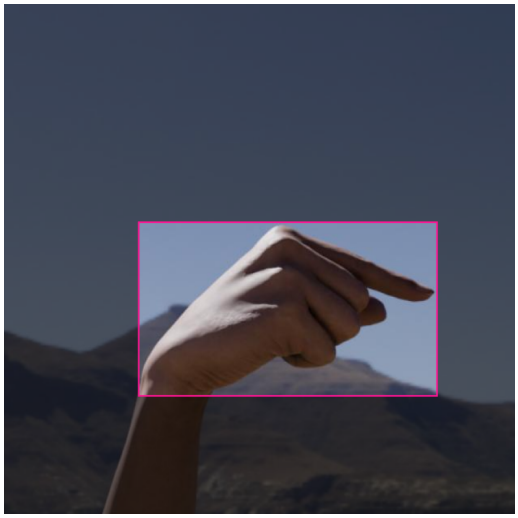

- **MyLeft, MyRight, YourLeft, YourRight Hands Detection** — https://universe.roboflow.com/sonu-frtzd/hands-lakl8-lyl74/dataset/1

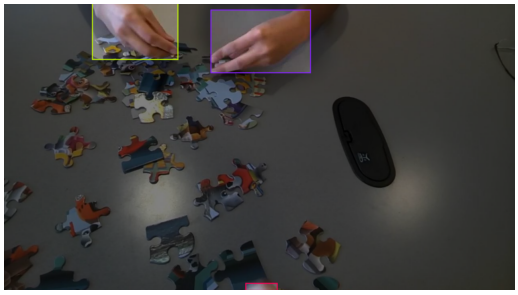

The training configuration used default YOLOv8 hyperparameters with image size 640 × 640, batch size 16, and learning rate 1×10^{-3}. The Nano variant was chosen for faster convergence and inference speed on limited hardware.

```
Epoch    GPU_mem   box_loss   cls_loss   dfl_loss  Instances       Size
 1/20      7.51G      1.249      1.614      1.389         33        640: 100% ──────────── 233/233 0.8it/s 4:44
           Class     Images  Instances      Box(P          R      mAP50  mAP50-95): 100% ──────────── 20/20 0.8it/s 26.4s
             all       2480       3495      0.833      0.821       0.86      0.529

Epoch    GPU_mem   box_loss   cls_loss   dfl_loss  Instances       Size
 2/20      7.13G      1.227      1.057      1.355         34        640: 100% ──────────── 233/233 0.9it/s 4:31
           Class     Images  Instances      Box(P          R      mAP50  mAP50-95): 100% ──────────── 20/20 0.8it/s 25.6s
             all       2480       3495      0.724      0.729       0.748      0.462

Epoch    GPU_mem   box_loss   cls_loss   dfl_loss  Instances       Size
 3/20      7.15G      1.237     0.9897      1.365         40        640: 100% ──────────── 233/233 0.9it/s 4:29
           Class     Images  Instances      Box(P          R      mAP50  mAP50-95): 100% ──────────── 20/20 0.8it/s 24.9s
             all       2480       3495      0.758      0.722       0.799      0.466

Epoch    GPU_mem   box_loss   cls_loss   dfl_loss  Instances       Size
 4/20      7.17G       1.19     0.9092      1.328         35        640: 100% ──────────── 233/233 0.9it/s 4:25
           Class     Images  Instances      Box(P          R      mAP50  mAP50-95): 100% ──────────── 20/20 0.8it/s 26.6s
             all       2480       3495      0.742      0.803       0.826      0.536

Epoch    GPU_mem   box_loss   cls_loss   dfl_loss  Instances       Size
 5/20      7.18G      1.137     0.8286      1.298         54        640: 100% ──────────── 233/233 0.9it/s 4:33
           Class     Images  Instances      Box(P          R      mAP50  mAP50-95): 100% ──────────── 20/20 0.8it/s 25.6s
             all       2480       3495       0.88      0.858       0.912      0.606

Epoch    GPU_mem   box_loss   cls_loss   dfl_loss  Instances       Size
 6/20       7.2G      1.097     0.7769      1.268         30        640: 100% ──────────── 233/233 0.9it/s 4:31
           Class     Images  Instances      Box(P          R      mAP50  mAP50-95): 100% ──────────── 20/20 0.8it/s 26.0s
             all       2480       3495      0.919       0.92       0.963      0.696

Epoch    GPU_mem   box_loss   cls_loss   dfl_loss  Instances       Size
 7/20      7.22G      1.059     0.7354      1.244         39        640: 100% ──────────── 233/233 0.9it/s 4:30
           Class     Images  Instances      Box(P          R      mAP50  mAP50-95): 100% ──────────── 20/20 0.8it/s 26.2s
             all       2480       3495      0.917       0.92       0.961      0.692

Epoch    GPU_mem   box_loss   cls_loss   dfl_loss  Instances       Size
 8/20      7.24G      1.038     0.6996      1.228         54        640: 100% ──────────── 233/233 0.9it/s 4:30
           Class     Images  Instances      Box(P          R      mAP50  mAP50-95): 100% ──────────── 20/20 0.8it/s 24.0s
             all       2480       3495      0.941      0.941       0.975      0.728

Epoch    GPU_mem   box_loss   cls_loss   dfl_loss  Instances       Size
 9/20      7.25G      1.024     0.6809      1.221         34        640: 100% ──────────── 233/233 0.9it/s 4:20
           Class     Images  Instances      Box(P          R      mAP50  mAP50-95): 100% ──────────── 20/20 0.8it/s 25.2s
             all       2480       3495      0.943      0.936       0.975       0.72

Epoch    GPU_mem   box_loss   cls_loss   dfl_loss  Instances       Size
10/20      7.27G      0.989     0.6526      1.204         46        640: 100% ──────────── 233/233 0.9it/s 4:24
           Class     Images  Instances      Box(P          R      mAP50  mAP50-95): 100% ──────────── 20/20 0.8it/s 24.6s
             all       2480       3495      0.934      0.944       0.974      0.698
```

Figure 3.2: Training Epochs

3.4 Results and Analysis

We evaluated the approach qualitatively on multiple images. Figure 3.3 presents seven representative results showing:

- The original image,
- The seed initialization (YOLO bounding box in blue, foreground seed box in green, and sampled background points in red),
- The final segmented hand output.

Performance observations:

- The pipeline performs well when the hand is clearly distinguishable from the background (good color contrast).
- Failure occurs when the background has colors or textures similar to the hand, since GrabCut is fundamentally a color-based algorithm.
- The method provides a balance between speed and quality without requiring pixel-level ground truth labels for training.

3.5 Discussion

This hybrid approach demonstrates how detection and segmentation can be combined efficiently. The YOLO detector provides robust localization, while GrabCut refines the region based purely on color distributions. Although it lacks the semantic robustness of deep segmentation networks (e.g., RefineNet or DeepLab), it is computationally lightweight and effective for real-time applications with moderate constraints.

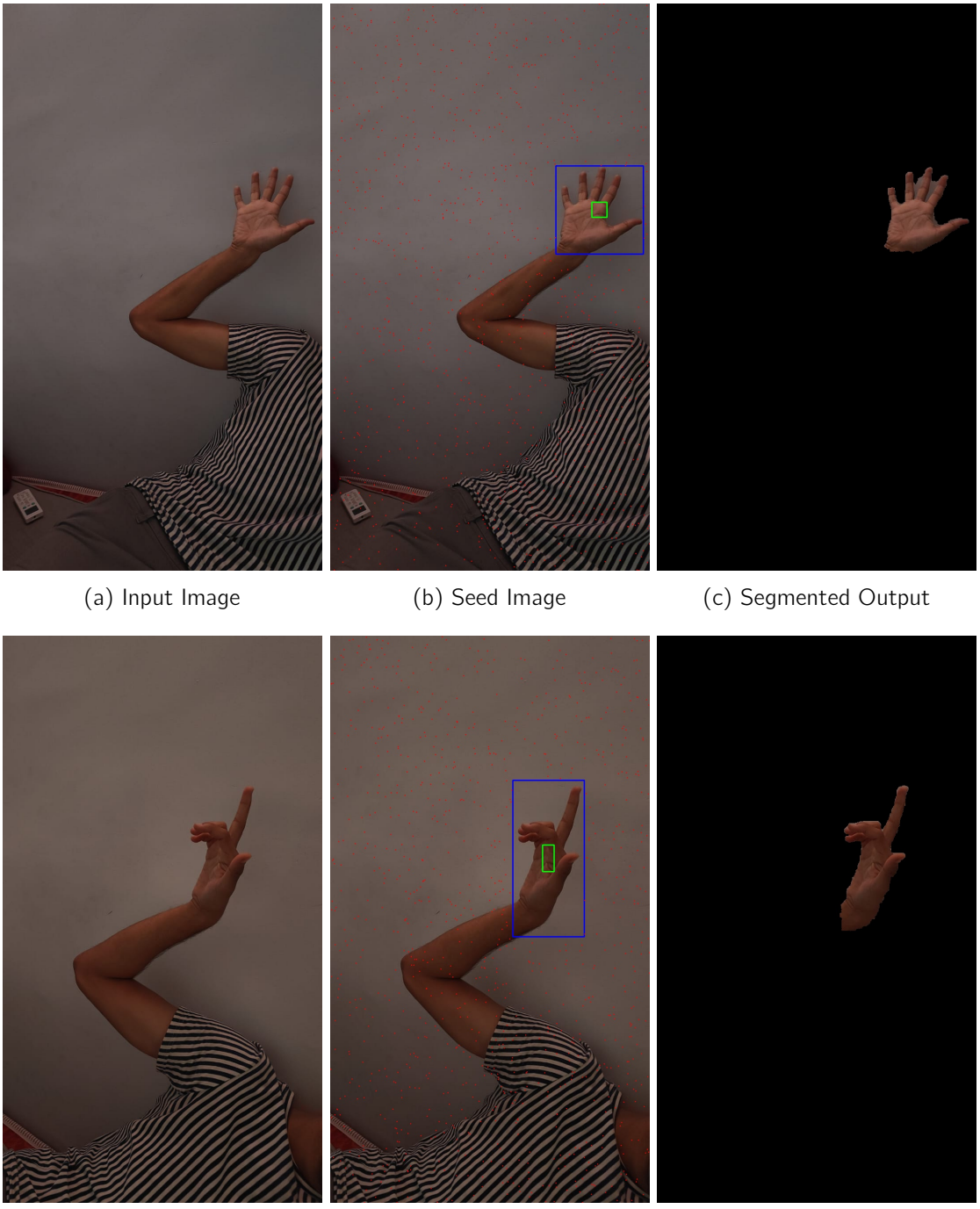

(a) Input Image (b) Seed Image (c) Segmented Output

(d) Input Image (e) Seed Image (f) Segmented Output

Figure 3.3: Sample results from the YOLOv8 + GrabCut pipeline

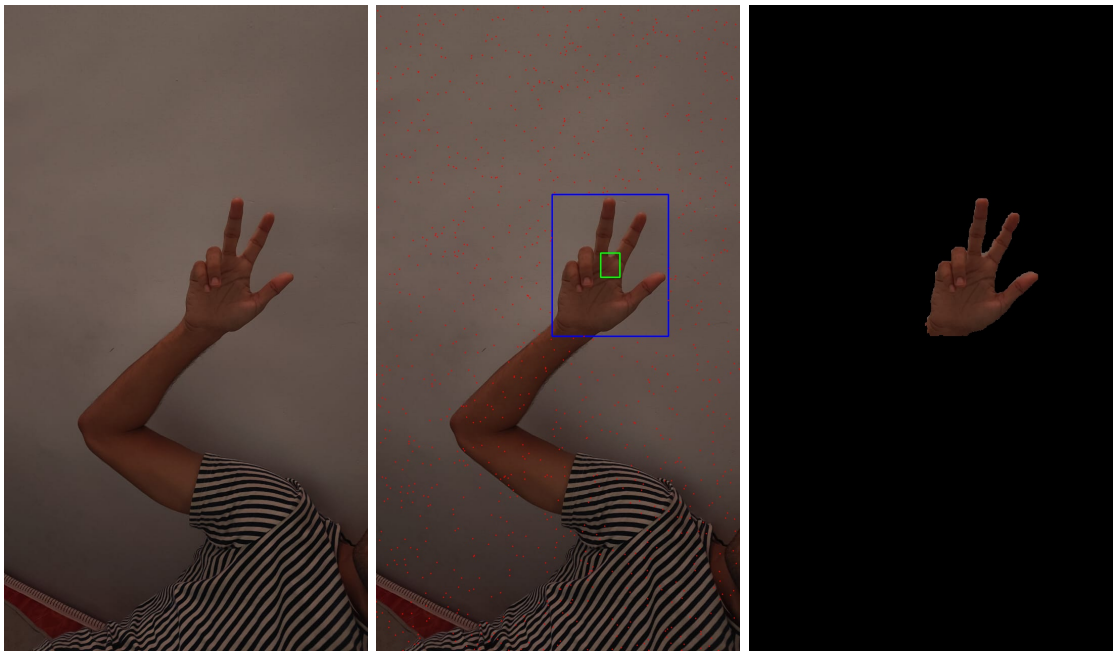

(g) Input Image (h) Seed Image (i) Segmented Output

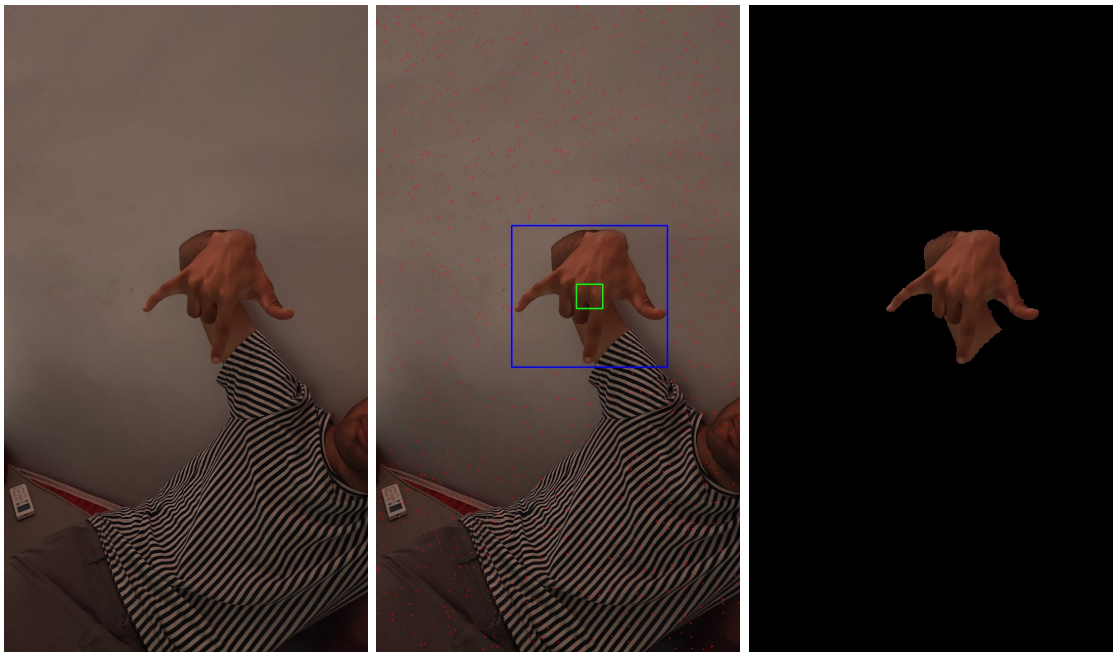

(j) Input Image (k) Seed Image (l) Segmented Output

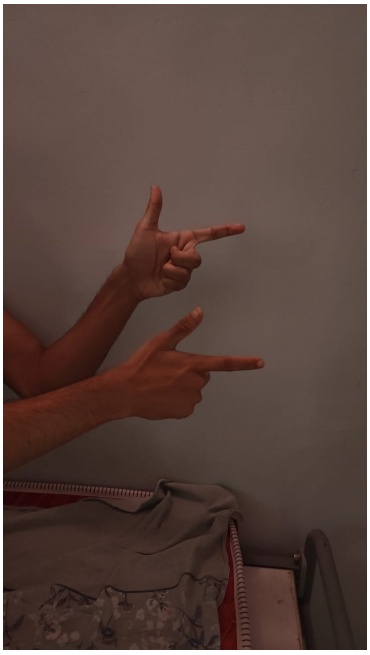
(m) Input Image

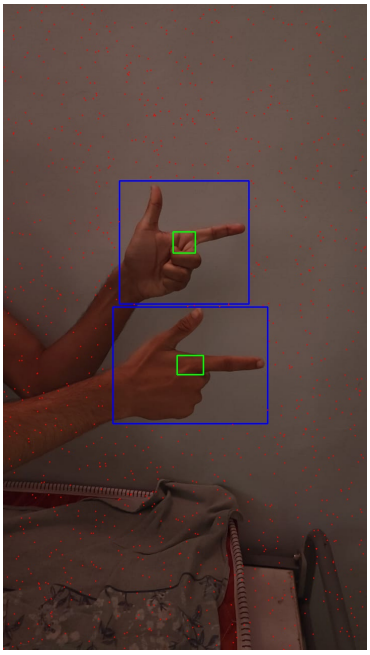
(n) Seed Image

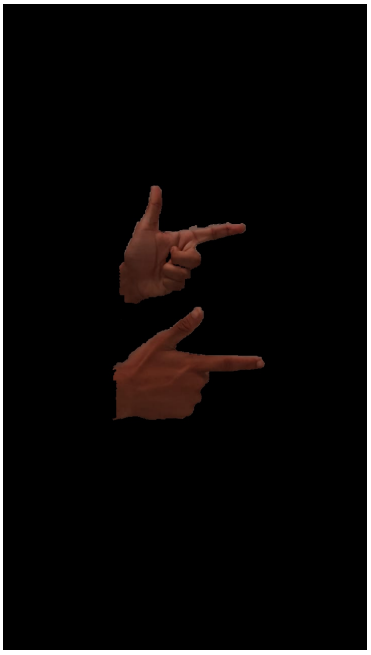
(o) Segmented Output


(p) Input Image

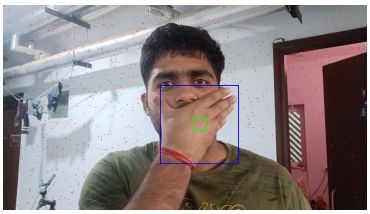
(q) Seed Image


(r) Segmented Output

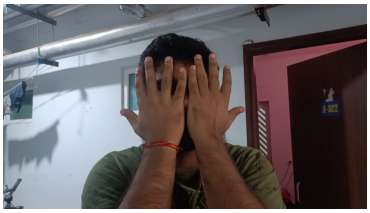
(s) Input Image

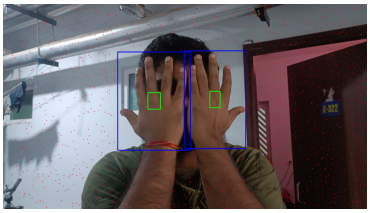
(t) Seed Image

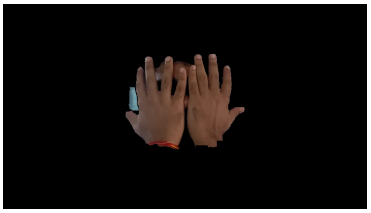
(u) Segmented Output

Chapter 4

RefineNet Implementation

This chapter describes the complete end-to-end implementation of the original research paper *"Analysis of Hand Segmentation in the Wild"* by Aisha Urooj Khan and Ali Borji. The work replicates the full pipeline using the **RefineNet-Res101** architecture for pixel-level hand segmentation, including pretraining on the Pascal Person-Part dataset, followed by fine-tuning on various hand segmentation datasets.

The entire process was computationally intensive and required several optimization and infrastructure decisions to make training feasible. This chapter explains each step, challenges faced, results obtained, and performance comparisons.

4.1 Overview of the Implementation Pipeline

The overall implementation followed these key stages:

1. Extraction and preprocessing of the Pascal Parts dataset (from MATLAB annotations to segmentation masks).
2. Training RefineNet-Res101 on Pascal Parts dataset to obtain pretrained weights.
3. Fine-tuning the pretrained model on the four hand segmentation datasets:
    - EgoHands
    - EgoYouTubeHands (EYTH)
    - GTEA
    - HandOverFace (HOF)
4. Evaluation using cross-dataset mean Intersection-over-Union (mIoU), mean Recall, and mean Precision.
5. Comparison of results using two different batch sizes (4 and 16).

4.2 Step 1: Pretraining on Pascal Parts Dataset

4.2.1 Data Extraction and Preprocessing

The Pascal Person-Part dataset consists of 21 semantic categories including human parts such as torso, arms, legs, and hands. However, the annotations are stored in `.mat` files which contain pixel-wise label maps.

To prepare the data:

1. Loaded each `.mat` annotation file.
2. Extracted the segmentation mask corresponding to the 21 semantic classes.
3. Saved both the RGB image and the corresponding mask image as `.png` files in structured directories.

Figure 4.1: 21-class Mask

This step was essential since pretrained RefineNet weights for Pascal Parts were not publicly available. Hence, the model had to be trained from scratch.

4.2.2 Pretraining Setup

- **Architecture:** RefineNet-Res101.
- **Number of classes:** 21.
- **Optimizer:** Adam with learning rate 5×10^{-5}.
- **Loss function:** CrossEntropyLoss.

Challenge: Training the full RefineNet architecture on Pascal Parts took approximately **5 hours per epoch** on a single T4 GPU. To overcome this limitation, training was distributed using **Lightning AI** for managing GPU workloads efficiently and to enable resumable training with checkpoints.

4.3 Step 2: Fine-Tuning on Hand Segmentation Datasets

After obtaining the pretrained model from Pascal Parts, the weights were fine-tuned on four specific datasets: EgoHands, EYTH, GTEA, and HandOverFace. Each dataset was trained individually while maintaining the same architecture and training settings.

4.3.1 Training Details

- **Input size:** 512×512
- **Optimizer:** Adam
- **Learning rate:** 1×10^{-4}
- **Batch sizes:** 4 and 16 (for performance comparison)
- **Loss:** Binary Cross Entropy (Hand vs. Background)
- **Evaluation:** mIoU, mPrecision, mRecall (on all datasets and cross-dataset)

4.3.2 Batch Size Comparison

Two sets of experiments were performed to study the effect of batch size:

Batch Size = 4: Training was more stable but generalization was weaker. The mIoU values were comparatively lower on cross-dataset evaluation.

Batch Size = 16: Higher batch size improved stability and overall accuracy. The model converged faster and produced results closer to the original paper.

4.4 Step 3: Cross-Dataset Evaluation

Trained on ↓	EgoHands	EYTH	GTEA	HOF	Combined
EgoHands	0.8603 / 0.9156 / 0.9343	0.2190 / 0.4496 / 0.2993	0.7342 / 0.8350 / 0.8589	0.4149 / 0.7272 / 0.4914	0.7580 / 0.8733 / 0.8517
EYTH	0.3976 / 0.4510 / 0.7704	0.6033 / 0.7057 / 0.8061	0.2970 / 0.3047 / 0.9208	0.2322 / 0.2729 / 0.6091	0.3794 / 0.4243 / 0.7819
GTEA	0.4139 / 0.5678 / 0.6043	0.1632 / 0.1973 / 0.4861	0.7909 / 0.8279 / 0.9466	0.1182 / 0.1437 / 0.3991	0.4451 / 0.5779 / 0.6595
HOF	0.4484 / 0.5757 / 0.6698	0.2616 / 0.3293 / 0.5600	0.5386 / 0.5771 / 0.8898	0.6960 / 0.8068 / 0.8351	0.4682 / 0.5794 / 0.7092

Table 4.1: Cross-dataset performance (Batch Size = 16). Each cell shows (mIoU / mRec / mPrec).

Trained on ↓	EgoHands	EYTH	GTEA	HOF	Combined
EgoHands	0.8603 / 0.9156 / 0.9343	0.2190 / 0.4496 / 0.2993	0.7342 / 0.8350 / 0.8589	0.4149 / 0.7272 / 0.4914	0.7580 / 0.8733 / 0.8517
EYTH	0.2471 / 0.2634 / 0.7999	0.6356 / 0.6974 / 0.8776	0.1292 / 0.1313 / 0.8906	0.1217 / 0.1322 / 0.6047	0.2346 / 0.2484 / 0.8076
GTEA	0.3104 / 0.4315 / 0.5251	0.0377 / 0.0665 / 0.0800	0.7824 / 0.8339 / 0.9269	0.0680 / 0.1523 / 0.1094	0.3416 / 0.4755 / 0.5482
HOF	0.4383 / 0.6357 / 0.5853	0.2618 / 0.3765 / 0.4620	0.4100 / 0.4387 / 0.8623	0.7216 / 0.8410 / 0.8357	0.4406 / 0.6016 / 0.6221

Table 4.2: Cross-dataset performance (Batch Size = 4). Each cell shows (mIoU / mRec / mPrec).

Key Observations:

- **Batch size 16** provided higher mIoU and more stable cross-dataset generalization.
- The model trained on **EgoHands** achieved the best overall accuracy, while **EYTH-trained models** generalized better to unseen datasets.
- Models trained on **HOF** performed well on occluded and face-hand overlap cases.
- Small datasets (like GTEA) showed weaker cross-dataset performance due to limited variability.

4.5 Step 4: Visual Results

Qualitative observations:

- The segmentation maps closely match the ground truth for clear, well-lit hand regions.
- The model generalizes across varied hand orientations and lighting.
- Minor mis-segmentations occur when hands are motion-blurred or partially occluded by objects.

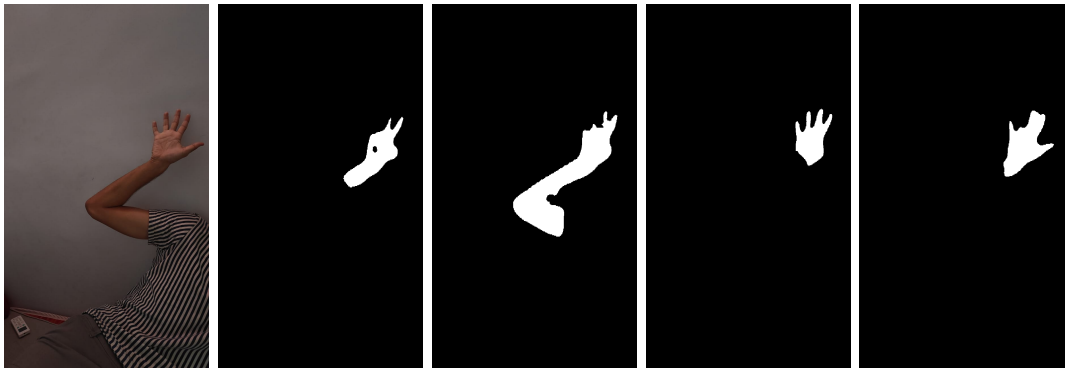

(a) Original (b) EgoHands (c) GTEA (d) EYTH (e) HoF

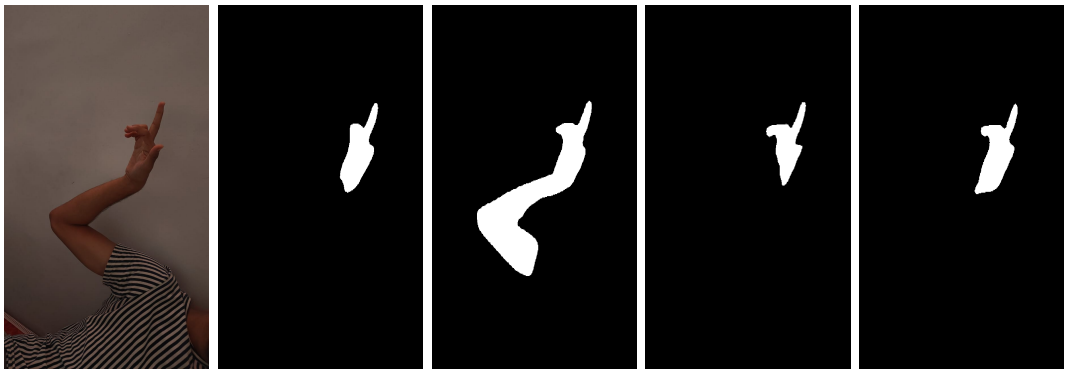

(f) Original (g) EgoHands (h) GTEA (i) EYTH (j) HoF

(k) Original (l) EgoHands (m) GTEA (n) EYTH (o) HoF

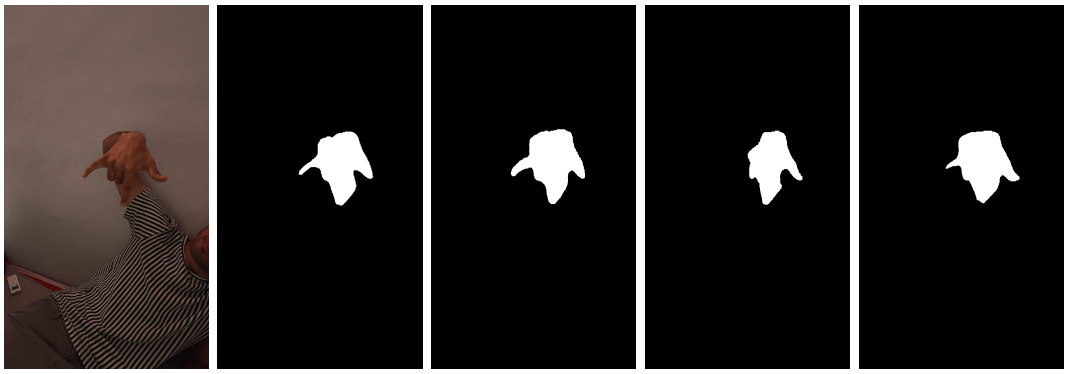

(p) Original (q) EgoHands (r) GTEA (s) EYTH (t) HoF

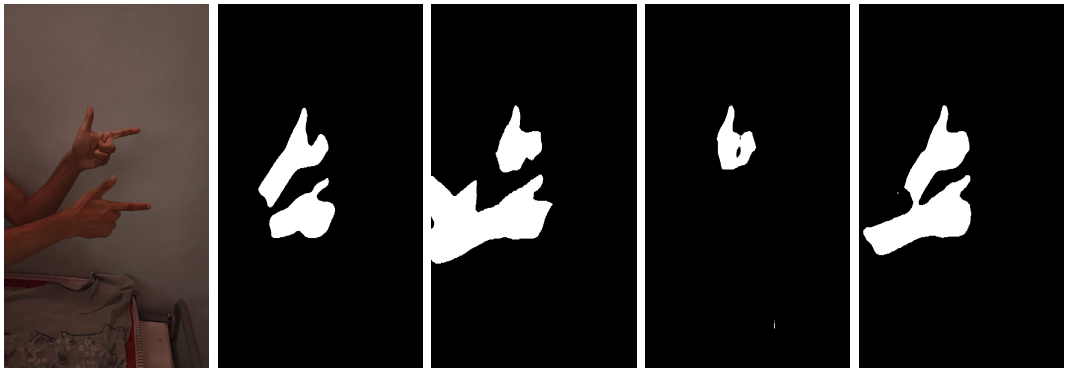

(u) Original (v) EgoHands (w) GTEA (x) EYTH (y) HoF

(z) Original () EgoHands () GTEA () EYTH () HoF

() Original () EgoHands () GTEA () EYTH () HoF

4.6 Challenges Faced

- **Unavailable pretrained weights:** Required manual training on Pascal Parts, which was time-consuming.
- **High computation cost:** RefineNet is a deep, multi-stage architecture. Training required ∼5 hours per epoch on Google Colab's T4 GPU, ∼2.6 hours per epoch on an A100 GPU, and only ∼5 minutes per epoch on an H200 GPU (accessible by creating multiple Colab accounts to obtain H200 sessions).
- **Cross-dataset variability:** Significant performance drops when testing on datasets with different illumination and camera perspectives.

4.7 Conclusion

This experiment successfully replicates the original research paper, confirming that:

- RefineNet remains one of the most effective architectures for pixel-level hand segmentation.
- Training from scratch on Pascal Parts and fine-tuning on smaller datasets can achieve comparable results to reported benchmarks.
- Batch size significantly influences generalization and stability.

The complete pipeline, though resource-intensive, validates the core contributions of the original paper, and demonstrates the feasibility of reproducing large-scale hand segmentation in realistic environments.